AIMS Mathematics

https://www.aimspress.com/journal/Math

AIMS Mathematics, 11(8): 26077–26096.
DOI:10.3934/math.20261044
Received: 28 April 2026
Revised: 18 June 2026
Accepted: 28 July 2026
Published: 20 August 2026

Research article

A high-order ERK-SUPG method with Said-Ball elements for modeling convection-dominated flows

Lanyin Sun* **and Ziwei Dong**

School of Mathematics and Statistics, Xinyang Normal University, Xinyang, China

* **Correspondence:** Email: lysun@xynu.edu.cn.

Abstract: This paper develops a high-order explicit Runge-Kutta streamline upwind/Petrov-Galerkin (ERK-SUPG) method to simulate convection-dominated flows in offshore hydrocarbon reservoir development. The method integrates explicit Runge-Kutta temporal discretization with a streamline upwind/Petrov-Galerkin spatial scheme based on Said-Ball basis functions, ensuring numerical stability and avoiding oscillations in high-order computations. Numerical results demonstrate that the ERK-SUPG method, with stabilization parameters dependent on time and spatial step sizes, achieve theoretical convergence rates of $O(h^{2(q+1)/3} + \tau^p)$ and $O(h^{q+1/2} + \tau^p)$, respectively. Numerical tests on reservoir-scale models, including scenarios with time-dependent convection and mixed boundary conditions, show errors reduced to 10^{-11} under mesh refinement, validating the method's robustness and effectiveness for subsea fluid migration analysis.

Keywords: offshore hydrocarbon reservoir development; convection-dominated equations; ERK method; SUPG method
Mathematics Subject Classification: 65D17, 65M60

1. Introduction

With the growing global energy demand and increasing strategic importance of offshore hydrocarbon resources [1–3], the efficient development of reservoirs has become a critical focus. The convection-diffusion-reaction (CDR) equations serve as the fundamental equations for characterizing the dynamic processes of fluid flow, diffusion, and physicochemical interactions [4, 5]. Consider the following CDR equations with disjoint Dirichlet Γ_D and Neumann Γ_N boundaries ($\Gamma = \Gamma_D \cup \Gamma_N$) in $\Omega \in \mathbb{R}^2$ and the time interval $[0, T]$:

$$u_t - \varepsilon\Delta u + \mathbf{b} \cdot \nabla u + cu = f, \qquad \text{in } \Omega \times [0, T], \tag{1.1a}$$

$$u = \alpha, \qquad \text{in } \Omega \text{ and at } t = 0, \tag{1.1b}$$

$$u = g_D, \qquad \text{on } \Gamma_D \times [0, T], \tag{1.1c}$$

$$\nabla u \cdot \mathbf{n} = g_N, \qquad \text{on } \Gamma_N \times [0, T], \tag{1.1d}$$

where u is the hydrocarbon concentration; $\varepsilon > 0$ is the constant diffusion coefficient, representing the combined effect of the molecular diffusion and mechanical dispersion in offshore hydrocarbon reservoirs; $\mathbf{b} = (b_1, b_2)$ is the convection coefficient, characterizing the macroscopic flow field of oil, gas, and water in offshore reservoirs; c is the reaction coefficient, quantifying the rate of physicochemical reactions; α is the initial value; $\mathbf{n}$ is the outward normal unit vector; and f is the source term.

Obtaining the analytical solution of CDR equations is quite challenging, and many scholars have conducted research on analytical solutions for CDR equations. Kim [6] obtained the general one-dimensional (1D) analytical solution of CDR-source equations. Askar et al. [7] employed the travelling-wave Ansatz to derive the new analytical solution for diffusion-reaction equations. Further, various numerical methods have been employed to solve the equations, such as the finite element method (FEM) [8] and the finite volume method [9].

The FEM is a widely adopted numerical technique for spatial discretization, forming the foundation for obtaining computationally tractable solutions. In 2003, Lewis et al. [10] used the FEM to establish a numerical model of the Ekofisk field, yielding seabed subsidence contours consistent with past bathymetric surveys. In 2018, Dunham et al. [11] applied a 3D marine controlled-source electromagnetic finite-element forward modeling method to marine hydrocarbon reservoir exploration. In 2022, Allawi and Al-Jawad [12] built 4D finite element modeling to analyze stress redistribution in depleted reservoirs using well data.

During the offshore hydrocarbon reservoir development, convection-dominated behavior is particularly prevalent in fluid migration processes [13]. The high-pressure and high-flow-rate conditions of offshore reservoirs result in the convection term being much larger than the diffusion term. Traditional FEM often produces numerical oscillations in such cases, making it difficult to obtain accurate solutions and reducing the reliability of numerical simulations. To ensure stability, the stabilized FEM are usually employed, such as the streamline upwind/Petrov-Galerkin (SUPG) method [14] and Galerkin least squares method [15].

The SUPG method provides reliable support for the simulation of convection-dominated fluid migration. In 1982, Brooks and Hughes [16] proposed the streamline upwind finite-element method for convection-dominated flows, extending optimal upwind schemes to multidimensional problems. In 1987, SUPG-based finite-element procedures for time-dependent CDR equations were developed by Tezduyar et al. [17] to numerically simulate single-well chemical tracer tests for measuring remaining oil in depleted fields. In 2011, John and Novo [18] solved convection-dominated CDR equations using the SUPG method, along with the backward Euler and Crank-Nicolson (CN) methods. In 2025, Esmaily and Jia [19] presented a novel stabilized approach, augmented SUPG, a consistent weighted residual method with two complex-valued stabilization parameters.

In FEM, Lagrange polynomials [20] and Hermite polynomials [21] are often used as interpolation basis functions. They share the drawback of exhibiting the Runge phenomenon in high-degree calculations [22]. However, polynomial basis functions do not have this drawback. Ball basis functions are a typical type of polynomial basis functions [23] which possess properties such as the ability to approximate complex functions [24], which enables them to serve as basis functions in FEM. In 2004, dual bases for a K-parameterized generalized Ball curve family were presented by Wu [25]. In 2009, Zhang et al. [26] introduced the dual bases for Wang-Bézier curves parameterized by the position parameter L. In 2023, Hu et al. [23] constructed a new type of combined cubic generalized Ball surfaces and explored their shape optimization. A novel approach was proposed by Hu et al. [27] in 2025 for solving the degree reduction problem of ball Said-Ball surfaces.

For the temporal discretization of time-dependent partial differential equations (PDEs), both the θ-method [28] and the explicit Runge-Kutta (ERK) method [29] are widely used discretization methods. In [18], which focus on solving the convection-dominated equations, two forms of the θ-method (namely the backward Euler method with $\theta = 1$ and the CN method with $\theta = 0.5$) were employed for solutions. However, compared with the θ-method, the ERK method exhibits distinct advantages in solving time-dependent PDEs. First, the ERK method offers higher temporal accuracy: The θ-method is typically limited to 1-order accuracy ($\theta \neq 0.5$) or 2-order accuracy ($\theta = 0.5$) [30], whereas the ERK method can achieve 3-order, 4-order, or even higher accuracy [31]. Second, the ERK method provides better stability: The stability of the θ-method is highly dependent on the choice of θ and is often restricted to small time steps [32], whereas the ERK method possesses strong stability properties [33, 34], allowing for larger time steps.

Therefore, in this paper, the RK method is selected as the temporal discretization for convection-dominated equations. Runge [35] was the first to present a 2-order RK method by combining a sequence of Euler formulas. The implicit RK (IRK) method was proposed by Butcher [36] in 1964. In 1977, Alexander [37] focused on diagonally IRK methods, exploring their construction, properties, order, and stability in solving stiff ordinary differential equations. In 2013, Dimarco and Pareschi [38] examined implicit-explicit RK methods for stiff Boltzmann-type kinetic equations. A new class of fractional order RK methods for approximating solutions to fractional differential equations was presented by Ghoreishi et al. [39] in 2023.

In this work, we develop an ERK-SUPG method for convection-dominated equations. Following the stabilized framework in [18], we employ the SUPG method but use Said-Ball basis functions for spatial discretization. For temporal discretization, we replace the θ-method with a more accurate and stable ERK method. Compared with earlier θ-FEM using Wang-Ball basis functions [40], the proposed approach not only incorporates SUPG stabilization to suppress oscillations in strongly convective problems but also improves temporal accuracy via ERK method. Numerical examples verify the effectiveness of the ERK-SUPG method.

This paper is structured in the following manner: In Section 2, we present the definition of the Said-Ball element on a rectangular mesh subdivision. In Section 3, we construct the trial and test function spaces using Said-Ball basis functions and propose an ERK-SUPG method to solve convection-dominated equations. In Section 4, by solving different convection-dominated equations, we conclude that this method is effective in solving these equations through the analysis of errors and convergence orders. In Section 5, we provide a summary of the work presented herein and offer outlooks on subsequent research directions.

2. Said-Ball elements

This section introduces the Said-Ball basis functions, which can be used as the basis functions of the SUPG method.

First, we present the definition of the Said-Ball basis functions.

Definition 1. *[27] In 1D space, the n degree Said-Ball basis functions are defined as follows:*

$$B_i^n(x) = \begin{cases} \binom{\lfloor n/2 \rfloor + i}{i} x^i (1-x)^{\lfloor n/2 \rfloor + 1}, & 0 \le i \le \lceil n/2 \rceil - 1, \\ \binom{n}{n/2} x^{\lfloor n/2 \rfloor} (1-x)^{\lfloor n/2 \rfloor}, & i = \lfloor n/2 \rfloor, \\ B_{n-i}^n (1-x), & \lfloor n/2 \rfloor + 1 \le i \le n, \end{cases}$$

where $x \in [0, 1]$, $\lfloor n/2 \rfloor$ *is the floor function, and* $\lceil n/2 \rceil$ *is the ceiling function.*

We respectively present the graphs of Said-Ball basis functions of degree 2 and 4 in the two subfigures of Figure 1. Next, we present their properties.

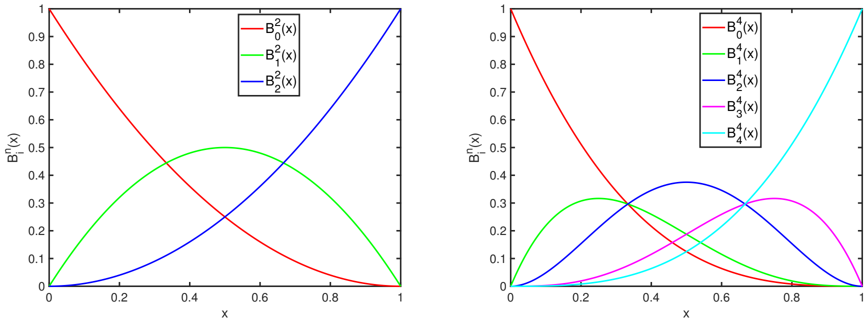

(a) Said-Ball basis functions of degree 2 (b) Said-Ball basis functions of degree 4

Figure 1. Said-Ball basis functions.

Property 1. *[41] For* $x \in [0, 1]$, *the properties of Said-Ball basis functions for* $i = 0, 1, \cdots, n$ *are as follows:*

1) *Positivity:* $0 \le B_i^n(x) \le 1$.
2) *Partition of unity:* $\sum_{i=0}^{n} B_i^n(x) = 1$.
3) *Recursion:* $B_i^{2n+1}(x) = B_i^{2n}(x), B_{2n+1-i}^{2n+1}(x) = B_{2n-i}^{2n}(x), 0 \le i \le n-1; B_n^{2n}(x) = B_n^{2n+1}(x) + B_{n+1}^{2n+1}(x)$.

Then, we introduce several necessary background concepts. First, the finite element is a core tool for discretizing regions in the numerical simulation. Let Ω_h be a rectangular partition of the 2D domain Ω. We present the definition of a finite element [42]: If

- M is a rectangular finite element subdomain of Ω_h.
- $\mathcal{Q}$ is the finite-dimensional shape function space restricted to the element M.
- $\mathcal{D} = \{D_1, D_2, \cdots, D_k\}$ denotes the set of local degrees of freedom (DoFs) of the element M.

We say $(M, \mathcal{Q}, \mathcal{D})$ is a finite element.

Next, we take a single rectangular finite element M to illustrate the mesh structure and related definitions, as shown in Figure 2. For M, h_{M} stands for the element diameter, and $h = \max_{M \in \Omega_h} h_{\mathrm{M}}$ is the global mesh size. Let B_{M} be the largest inscribed sphere of M with diameter d_{M}. All meshes adopted in this work are regular: For each element M, there exists a constant $\beta \in (0, 1]$ such that $d_{\mathrm{M}} \ge \beta h_{\mathrm{M}}$. This regularity condition effectively prevents numerical errors induced by mesh distortion.

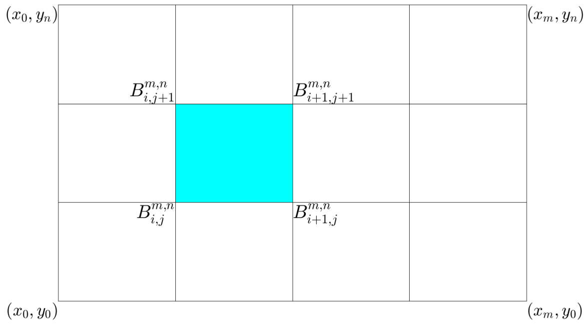

Figure 2. A rectangular mesh subdivision Ω_h.

In addition, $B^{m,n}_{i,j}$ denotes the piecewise tensor-product basis functions defined over the entire rectangular element M. The set of DoF $\mathcal{D} = \{D_{i,j}\}^{m,n}_{i,j=0}$ is in one-to-one correspondence with the internal nodes $\{(x_i, y_j) : i = 0, 1, \cdots, m, \ j = 0, 1, \cdots, n\}$ of the element.

Based on the above content and for the tensor product Said-Ball basis functions $B^{m,n}_{i,j}(x, y) = B^m_i(x)B^n_j(y)\,(i = 0, 1, \cdots, m, \ j = 0, 1, \cdots, n)$, the definition of a Said-Ball element as follows.

Definition 2. *For $\Omega_h \in \mathbb{R}^2$, if the following hold:*

- *M is a rectangular element.*
- *$\mathcal{Q} = span\{B^{m,n}_{i,j}\}^{m,n}_{i,j=0}$.*
- *$\mathcal{D} = \{D_{i,j}\}^{m,n}_{i,j=0}$ is the DoFs,*

we say that $(M, \mathcal{Q}, \mathcal{D})$ is a Said-Ball element.

The following theorem illustrates the unisolvence of a Said-Ball element, ensuring that the element can provide a unique and reliable numerical solution when discretizing convection-dominated equations.

Theorem 1. *If $(M, \mathcal{Q}, \mathcal{D})$ is a Said-Ball element, then $\mathcal{D}$ is a basis of $\mathcal{Q}'$, where $\mathcal{Q}'$ is the dual space of $\mathcal{Q}$.*

Proof. For the rectangular element M, the tensor-product Said-Ball space $\mathcal{Q}$ satisfies $\dim \mathcal{Q} = (m + 1)(n + 1)$. The set $\mathcal{D}$ consists of nodal evaluation, and its cardinality is also $(m + 1)(n + 1)$, so their dimensions coincide.

Take any $q \in \mathcal{Q}$ vanishing at all nodal points in $\mathcal{D}$. Restricting q to any edge of M yields a univariate polynomial with all nodal points as zeros; hence, $q \equiv 0$ on M. Thus, the functionals in $\mathcal{D}$ are linearly independent. Because $\dim \mathcal{D} = \dim \mathcal{Q}$, $\mathcal{D}$ forms a basis of the dual space $\mathcal{Q}'$. □

In this section, we introduced Said-Ball elements, and in the next section, we will use them as the basis functions in the SUPG method to solve convection-dominated equations.

3. An high-order ERK-SUPG method

To overcome the difficulties of simulating fluid migration under convection-dominated scenarios, this section employs the SUPG and ERK methods to discretize spatial and temporal dimensions of convection-dominated equations, respectively.

3.1. A semi-discrete SUPG formulation

First, assuming Eq (1.1) satisfies that for $\forall\,(\mathbf{x},t)\in\Omega\times[0,T]$, $\exists\,\mu_0>0$ such that [43]

$$0<\mu_0\leq\mu(\mathbf{x},t)=(c-1/2\nabla\cdot\mathbf{b})\,(\mathbf{x},t). \tag{3.1}$$

For the domain Ω, we use $\|\cdot\|$ to represent the norm of $L^2(\Omega)$ and $|\cdot|_m$ to represent the semi-norm of $H^m(\Omega)$. Let $H^m(\Omega;0,T)=\{u(\cdot,t),u_t(\cdot,t)\in H^m(\Omega),\ \forall\,t\in[0,T]\}$, and $H_0^m(\Omega\setminus\Gamma_N)=\{u\in H^m(\Omega):u|_{\Gamma\setminus\Gamma_N}=0\}\in H^m(\Omega)$.

Let $(\cdot,\cdot)$ denote the inner product in $L^2(\Omega)$ and $(\cdot,\cdot)|_{\Gamma_N}$ denote the inner product on the boundary Γ_N. We then define

$$\begin{aligned} a(u,\gamma)&=(\varepsilon\nabla u,\nabla\gamma)+(\mathbf{b}\cdot\nabla u,\gamma)+(cu,\gamma),\\ b(\gamma)&=(f,\gamma)+(g_N,\gamma)|_{\Gamma_N}. \end{aligned}$$

Multiplying both sides of Eq (1.1a) and (1.1b) by the test function $\gamma\in H_0^1(\Omega)$, respectively, and then applying integration by parts, we obtain the following variational formulation: Find $u(\mathbf{x},t)\in H^1(\Omega;0,T)$ satisfying

$$\begin{cases}(u_t,\gamma)+a(u,\gamma)=b(\gamma), & \forall\gamma\in H_0^1(\Omega),\ t\in[0,T],\\ (u,\gamma)=(\alpha,\gamma), & \forall\gamma\in H_0^1(\Omega),\ t=0.\end{cases} \tag{3.2}$$

This formulation lays the foundation for the subsequent SUPG stabilized discretization tailored to offshore reservoir simulation scenarios.

In simulating convection-dominated fluid migration, the finite-dimensional function space Q is spanned by tensor product Said-Ball basis functions $B_{p,q}^{m,n}$ (Section 2). The basis functions are reindexed as ω_j $(j=1,\ldots,N_b)$ following the lexicographic order of the nodes $\{x_j\}_{j=1}^{N_b}$ in Ω_h (sorted by x- then y-direction). With $N_b=(m+1)(n+1)$ and each node x_j paired with ω_j, the space simplifies to

$$Q=\mathrm{span}\{\omega_j\}_j^{N_b}.$$

Using the Said-Ball basis function $\omega_j\,(j=1,\cdots,N_b)$, we can define the Said-Ball element subspace U_h:

$$U_h=\{u\in H^1(\Omega;0,T)\mid u|_{\mathrm{M}}\in Q,\ M\in\Omega_h\},$$

and $U_{h_0}=\{u\in U_h:u|_{\Gamma\setminus\Gamma_N}=0\}$.

To construct the semi-discrete SUPG formulation for simulating the convection-dominated fluid migration, stabilization terms are introduced based on the variational formulation (3.2) and adopt $\mathbf{b}\cdot\nabla\gamma$ as the test function. The test function $\mathbf{b}\cdot\nabla\gamma$ can adapt the numerical formulation to the nature of convection-dominated fluid transport.

Semi-discrete formulation: The semi-discrete SUPG formulation for Eq (1.1) is to find $u_h(\mathbf{x},t)\in H^1(U_h;0,T)=\{u_h(\mathbf{x},t),\ u_{h_t}(\mathbf{x},t)\in U_h,\forall\,t\in[0,T]\}$ such that

$$\begin{cases}(u_{h_t},\gamma)+a_{\mathrm{SUPG}}(u_h,\gamma)+\sum\limits_{M\in\Omega_h}\delta_{\mathrm{M}}(u_{h_t},\mathbf{b}\cdot\nabla\gamma)_{\mathrm{M}}=b(\gamma)+\sum\limits_{M\in\Omega_h}\delta_{\mathrm{M}}b(\mathbf{b}\cdot\nabla\gamma)_{\mathrm{M}},\ \forall\,\gamma\in U_{h_0},t\in[0,T],\\ (u_h,\gamma)=(\alpha,\gamma),\qquad \forall\gamma\in U_{h_0},t=0,\end{cases} \tag{3.3}$$

where

$$a_{\mathrm{SUPG}}(u_h,\gamma) = \varepsilon(\nabla u_h,\nabla\gamma) + (\mathbf{b}\cdot\nabla u_h,\gamma) + (cu_h,\gamma) + \sum_{M\in\Omega_h}\delta_{\mathrm{M}}(-\varepsilon\Delta u_h + \mathbf{b}\cdot\nabla u_h + cu_h, \mathbf{b}\cdot\nabla\gamma)_{\mathrm{M}},$$

and $b(\mathbf{b}\cdot\nabla\gamma) = (f,\mathbf{b}\cdot\nabla\gamma) + (g_N,\mathbf{b}\cdot\nabla\gamma)|_{\Gamma_N}$.

The following Lemma 1 demonstrates the coercivity of the SUPG bilinear form $a_{\mathrm{SUPG}}(\cdot,\cdot)$.

Lemma 1. *[43] Assume that the inequality (3.1) holds. Let δ_M be chosen such that*

$$\delta_M \le \frac{1}{2}\min\left\{\frac{h_M^2}{\varepsilon c_{inv}^2},\ \frac{\mu_0}{\|c\|_{M,\infty}^2}\right\};$$

then, $a_{SUPG}(\cdot,\cdot)$ satisfies

$$a_{SUPG}(u_h,u_h) \ge \frac{1}{2}\|u_h\|_{SUPG}^2$$

with

$$\|u_h\|_{SUPG} := \left(\varepsilon\|\nabla u_h\|^2 + \sum_{M\in\Omega_h}\delta_M\|\mathbf{b}\cdot\nabla u_h\|_M^2 + \|\mu^{\frac{1}{2}}u_h\|^2\right)^{\frac{1}{2}},$$

where c_{inv} is the coefficient of the inverse inequality $\|u_h\|_{l,p} \le c_{inv}h_M^{m-l-\frac{2}{p}-\frac{2}{q}}\|u_h\|_{m,q}$, $0\le m\le l$, $1\le p\le\infty$, and $1\le q\le\infty$.

Furthermore, the choice of the stabilization parameter δ_{M} in the SUPG formulation is guided by the work in [18]. It is demonstrated therein that when the convection coefficient is time-dependent, the stabilization parameter δ_{M} depends only on the time step, and when the convection coefficient is time-independent, the stabilization parameter δ_{M} exhibits two distinct cases of dependence, namely on the time step or the spatial mesh size.

The semi-discrete solution u_h of Eq (3.3) can be understood as an approximation of the exact solution u in a discrete spatial mesh. When the solution u_h is chosen in the Said-Ball element subspace U_h, by separating spatial and temporal variables, u_h can be expressed as

$$u_h(\mathbf{x},t) = \sum_{j=1}^{N_b} u_j(t)\omega_j(\mathbf{x}).$$

Next, we define the following three matrices: $\mathbf{M} = \left[\int_\Omega \omega_j\omega_i\,\mathrm{d}\Omega\right]_{i,j=1}^{N_b}$, $\mathbf{M}_{\mathrm{SUPG}} = \left[\int_\Omega \omega_j\omega_i\,\mathrm{d}\Omega + \sum_{M\in\Omega_h}\int_\Omega \delta_{\mathrm{M}}\omega_j\,\mathbf{b}\cdot\nabla\omega_i\,\mathrm{d}\Omega\right]_{i,j=1}^{N_b}$, $\mathbf{A}_{\mathrm{SUPG}}(t) = \left[\int_\Omega \varepsilon\nabla\omega_j\cdot\nabla\omega_i\,\mathrm{d}\Omega + \int_\Omega \mathbf{b}\cdot\nabla\omega_j\omega_i\,\mathrm{d}\Omega + \int_\Omega c\omega_j\omega_i\,\mathrm{d}\Omega + \sum_{S\in\Omega_h}\delta_{\mathrm{M}}\int_\Omega(-\varepsilon\Delta\omega_j + \mathbf{b}\cdot\nabla\omega_j + c\omega_j)\,\mathbf{b}\cdot\nabla\omega_i\,\mathrm{d}\Omega\right]_{i,j=1}^{N_b}$ and two vectors: $\mathbf{b}_{\mathrm{SUPG}}(t) = \left[\int_\Omega f\omega_i\,\mathrm{d}\Omega + \int_{\Gamma_N} g_N\omega_i\,\mathrm{d}s + \sum_{M\in\Omega_h}\int_\Omega \delta_{\mathrm{M}} f\,\mathbf{b}\cdot\nabla\omega_i\,\mathrm{d}\Omega\right]_{i=1}^{N_b}$, $\mathbf{V}(t) = [u_j(t)]_{j=1}^{N_b}$, thereby obtaining the vector form of the formulation (3.3):

$$\begin{cases}\mathbf{M}_{\mathrm{SUPG}}\mathbf{V}'(t) + \mathbf{A}_{\mathrm{SUPG}}(t)\mathbf{V}(t) = \mathbf{b}_{\mathrm{SUPG}}(t),\\ \mathbf{M}\mathbf{V}(0) = \displaystyle\int_\Omega \alpha\,\omega_i\,\mathrm{d}\Omega.\end{cases}\tag{3.4}$$

This subsection applied the SUPG method to spatially discretize convection-dominated equations. This method can effectively suppress numerical oscillations caused by convection dominance. The next subsection will proceed to discretize the temporal dimension.

3.2. *A full-discrete SUPG formulation*

Let $\tau = T/m$ be the time step size, where m is the number of time steps, and T denotes the simulation period. In the time interval $[0, T]$, the time nodes are represented as $t_i = i\,\tau\,(i = 0, 1, \cdots, m)$.

For simplicity, we denote

$$\mathbf{V}^i = \mathbf{V}(\mathbf{x}, t_i), \qquad \mathbf{V}^i_\tau = \frac{\mathbf{V}^i - \mathbf{V}^{i-1}}{\tau}.$$

Before introducing the ERK method, we present its corresponding Butcher tableau (i.e., Table 1), which directly determines the accuracy and stability of temporal discretization:

Table 1. The Butcher tableau.

$$\begin{array}{c|cccc} 0 & 0 & 0 & \cdots & 0 \\ c_2 & a_{21} & 0 & \cdots & 0 \\ \vdots & \vdots & \vdots & \ddots & \vdots \\ c_m & a_{m1} & a_{m2} & \cdots & 0 \\ \hline & b_1 & b_2 & \cdots & b_m \end{array}$$

where c_i, a_{ij} are independent of τ, $\sum_{j=1}^{m-1} a_{ij} = b_i\,(i = 2, 3, \cdots, m)$, and $\sum_{i=1}^{m-1} b_i = 1\,(b_i \geq 0)$.

We further set $\mathbf{b}^T = (b_1, b_2, \cdots, b_m)$, $\mathbf{1} = (1, 1, \cdots, 1) \in \mathbb{R}^m$ and

$$\mathbf{A} = \begin{pmatrix} 0 & 0 & \cdots & 0 \\ a_{21} & 0 & \cdots & 0 \\ \vdots & \vdots & \ddots & \vdots \\ a_{m1} & a_{m2} & \cdots & 0 \end{pmatrix}.$$

In addition, because $\mathbf{M}_{\text{SUPG}}$ and $\mathbf{M}$ are obviously invertible, Eq (3.4) can be transformed into the following form:

$$\begin{cases} \mathbf{V}'(t) = \mathcal{F}\left(\mathbf{V}(t), t\right), \\ \mathbf{V}(0) = \mathbf{M}^{-1} \displaystyle\int_\Omega \alpha\,\omega_i \,\mathrm{d}\Omega, \end{cases}$$

where

$$\mathcal{F}\left(\mathbf{V}(t), t\right) = \mathbf{M}^{-1}_{\text{SUPG}}\left(\mathbf{b}_{\text{SUPG}}(t) - \mathbf{A}_{\text{SUPG}}(t)\mathbf{V}(t)\right).$$

Thus, we use the m-stage p-order ERK method to discretize the time of Eq (3.4) and obtain the following full-discrete formulation. This formulation balances computational accuracy and efficiency.
Full-discrete SUPG formulation: The full-discrete SUPG formulation for Eq (1.1) is to find $\mathbf{V}^{n+1} \in H^1(U_h; 0, T)$ such that

$$\begin{cases} \mathbf{V}^{n+1} = \mathbf{V}^n + \tau \displaystyle\sum_{i=1}^m b_i k_i, \quad n = 0, 1, \cdots \\ \mathbf{V}(0) = \mathbf{M}^{-1} \displaystyle\int_\Omega \alpha\,\omega_i \,\mathrm{d}\Omega, \end{cases} \tag{3.5}$$

where $k_i = \mathcal{F}\left(\mathbf{V}^n + \tau \sum_{j=1}^{m-1} a_{ij}k_j, t_n + \tau c_i\right)$, and $\sum_{j=1}^{m-1} a_{ij} = b_i$. This is the standard recursive definition of ERK stage values, where each k_i is determined by the preceding stage terms k_j.

The coefficients b_i, c_i, and a_{ij} in the ERK method are determined according to the following principles: Taylor expansion is used to derive accuracy order conditions. This guarantees high-order consistency between the numerical solution $\mathbf{V}^{n+1}$ and the exact solution $u(\mathbf{x}, t_{n+1})$. For a s-stage ERK method of p-order accuracy, expand $\mathbf{V}^{n+1}$ and $u(\mathbf{x}, t_{n+1})$ into Taylor series at t_n. All coefficients of terms up to τ^p must be identical. Comparing terms of the same power yields the required conditions: For $m = 0, 1, \ldots, p$, conditions $\sum_{i=1}^{s} b_i c_i^m = 1/(m+1)$ and $\sum_{j=1}^{s} a_{ij} c_j^m = c_i^{m+1}/(m+1)$ [44] must be satisfied.

In the simulation of the convection-dominated flows, the stability of the numerical method is the core prerequisite for ensuring the reliability of concentration simulation results during long-term development. For the stability of the ERK method, [33] states that the amplification matrix is $R(z) = 1 + z\mathbf{b}^T(\mathbf{I} - z\mathbf{A})^{-1}\mathbf{1}$, where $z = -\lambda\tau$, and λ is the eigenvalue of $\mathbf{M}_{\text{SUPG}}^{-1}\mathbf{A}_{\text{SUPG}}$. The stability region of this method is derived by solving $G(z) \leq 1$. Furthermore, for the ERK method, the CFL condition [45] requires that the time step size τ be proportional to the mesh size h. Further, the proportionality constant C_{CFL} bounded by the stability radius of the ERK method. The specific form is as follows: $\tau \leq C_{CFL}h$, where C_{CFL} is related to the convective term coefficient and is independent of the mesh and time step sizes.

Error is the key indicator for quantifying the degree to which numerical solutions approximate the exact solutions, providing a basis for precision control in engineering simulations. As shown in [18], the convergence rate of the SUPG method is $O(h^{2(q+1)/3})$ and $O(h^{q+1/2})$, corresponding to the cases where the stabilization parameter depends on the time step and spatial step, respectively. Earlier we analyzed the principle for determining coefficients of the m-stage p-order ERK method; thus, the convergence rate of the ERK method is $O(\tau^p)$. Therefore, the convergence rate of the ERK-SUPG method is

$$\|\mathbf{V}^n - u(\mathbf{x}, t_n)\| \leq C\left(h^{2(q+1)/3} + \tau^p\right), \tag{3.6}$$

and

$$\|\mathbf{V}^n - u(\mathbf{x}, t_n)\| \leq C\left(h^{q+1/2} + \tau^p\right). \tag{3.7}$$

To make the overall convergence order reach the $(2(q+1)/3)$- or $(q+1/2)$-order, we can set $p \geq 2(q+1)/3$ or $q + 1/2$. Thus, p can be taken as $q + 1$.

In this section, an ERK-SUPG method was proposed to solve convection-dominated equations, aiming to reduce the numerical oscillation caused by the convection-dominated fluid. In the next section, we will use numerical examples related to offshore reservoir scenarios to illustrate the effectiveness of this method.

4. Numerical examples

This section presents three numerical examples to validate the effectiveness of the ERK-SUPG method for solving convection-dominated equations. The first example adopts Dirichlet boundary conditions and a time-independent convection field to test the basic behavior of the solution under steady driving effects, providing a standard benchmark for numerical validation. The second example applies Dirichlet boundary conditions with a time-dependent convection term to simulate unsteady flow evolution. The third example incorporates mixed Dirichlet-Neumann boundary conditions with a time-independent convection term, replicating realistic offshore reservoir scenarios.

Based on the analysis in the previous section, the optimal convergence order is obtained for $p = q + 1$. Thus, the order of the 7-stage ERK method used in this section is set to $p = q + 1$, where q denotes the degree of Said-Ball basis functions. Furthermore, all the errors in the calculations of this section are absolute errors, and all the calculations are performed using double-precision arithmetic.

Example 1. *This example constructs a benchmark model for hydrocarbon fluid migration under stable injection-production driving conditions in shallow-water offshore oilfields. In* $\Omega = [0, 1] \times [0, 1]$*, the convection term is* $\mathbf{b} = (1.3, 1.9)$ *and reflects the persistent high-velocity migration of convection-dominated fluids. The diffusion term retains a small coefficient* $\varepsilon = 10^{-6}$*. The reaction coefficient* $c = 1$ *quantifies the physicochemical interactions under stable flow conditions, and Dirichlet boundary conditions are uniformly applied to specify concentration constraints at boundaries. Furthermore, the exact solution is*

$$u(x, y, t) = txsin(2\pi x)sin(\pi y),$$

and the source term is

$$\begin{aligned} f(x, y, t) =& sin(2\pi x)sin(\pi y)\,(1.3t + tx + x) + 2.6tx\pi cos(2\pi x)sin(\pi y) \\ & - 10^{-6}\pi t sin(\pi y)(4cos(2\pi x) - 5x\pi sin(2\pi x)) + 1.9tx\pi cos(\pi y)sin(2\pi x). \end{aligned}$$

Following the analysis in [18], the stabilization parameter for time-independent convection can depend on both the time step τ *and spatial step h. In this example, we compute errors and convergence orders for both choices, as presented in Tables 2 and 3. Meanwhile, to more intuitively display the data in these tables, we plot the corresponding Figures 3 and 5 based on Tables 2 and 3, respectively.*

Table 2 presents the errors and convergence orders of the proposed ERK-SUPG method with stabilization parameter $\tau/9$*, and Table 3 shows corresponding results with* $\delta_M = h/5$*. Results from both tables demonstrate that as the degree of Said-Ball basis functions increases, the error decreases, and the convergence order improves, verifying that the scheme maintains stable accuracy under mesh refinement. Figures 3 and 5 visualize the results in Tables 2 and 3. A comparison between the convergence-order black lines and the error curves of the four norms clearly shows the enhanced convergence order of the proposed method.*

Table 2. The numerical errors in Example 1 by the ERK-SUPG method with $\delta_{\mathrm{M}} \sim \tau$.

Method	Mesh (h)	$\|\|\mathbf{V}^n - u(\mathbf{x}, t_n)\|\|$		$\|\mathbf{V}^n - u(\mathbf{x}, t_n)\|_1$		$\|\|\mathbf{V}^n - u(\mathbf{x}, t_n)\|\|_\infty$		$\|\|\mathbf{V}^n - u(\mathbf{x}, t_n)\|\|_{\mathrm{SUPG}}$	
		Error	Order	Error	Order	Error	Order	Error	Order
2×2 Said-Ball	$[\frac{1}{2}, \frac{1}{2}]$	3.75e-02	–	7.75e-01	–	9.98e-02	–	3.90e-02	–
	$[\frac{1}{4}, \frac{1}{4}]$	7.90e-03	2.25	2.70e-01	1.52	2.48e-02	2.01	8.34e-03	2.23
	$[\frac{1}{8}, \frac{1}{8}]$	1.87e-03	2.08	1.14e-01	1.24	6.61e-03	1.91	2.09e-03	2.00
3×3 Said-Ball	$[\frac{1}{2}, \frac{1}{2}]$	3.69e-02	–	5.96e-01	–	1.19e-01	–	3.74e-02	–
	$[\frac{1}{4}, \frac{1}{4}]$	1.49e-03	4.63	7.80e-02	2.93	3.59e-03	5.05	1.64e-03	4.51
	$[\frac{1}{8}, \frac{1}{8}]$	5.29e-05	4.82	6.84e-03	3.51	1.52e-04	4.56	7.15e-05	4.52
4×4 Said-Ball	$[\frac{1}{2}, \frac{1}{2}]$	3.65e-03	–	3.63e-02	–	5.97e-03	–	3.67e-03	–
	$[\frac{1}{4}, \frac{1}{4}]$	9.47e-05	5.27	1.05e-03	5.12	2.53e-04	4.56	3.94e-05	5.27
	$[\frac{1}{8}, \frac{1}{8}]$	3.07e-06	4.95	2.77e-05	5.24	7.50e-06	5.08	3.08e-06	4.95

Table 3. The numerical errors in Example 1 by the ERK-SUPG method with $\delta_{\mathrm{M}} \sim h$.

Method	Mesh (h)	$\|\mathbf{V}^n - u(\mathbf{x}, t_n)\|$		$\|\mathbf{V}^n - u(\mathbf{x}, t_n)\|_1$		$\|\mathbf{V}^n - u(\mathbf{x}, t_n)\|_\infty$		$\|\mathbf{V}^n - u(\mathbf{x}, t_n)\|_{\mathrm{SUPG}}$	
		Error	Order	Error	Order	Error	Order	Error	Order
2×2 Said-Ball	$[\frac{1}{2}, \frac{1}{2}]$	4.42e-02	–	6.49e-01	–	9.63e-02	–	2.70e-01	–
	$[\frac{1}{4}, \frac{1}{4}]$	7.43e-03	2.57	1.99e-01	1.70	2.30e-02	2.06	3.57e-02	2.25
	$[\frac{1}{8}, \frac{1}{8}]$	9.99e-04	2.89	5.48e-02	1.87	2.75e-03	3.06	1.12e-02	2.34
3×3 Said-Ball	$[\frac{1}{2}, \frac{1}{2}]$	1.06e-02	–	2.34e-01	–	2.45e-02	–	9.03e-02	–
	$[\frac{1}{4}, \frac{1}{4}]$	7.51e-04	3.82	3.69e-02	2.67	2.68e-03	3.19	1.05e-02	3.11
	$[\frac{1}{8}, \frac{1}{8}]$	4.49e-05	4.06	4.54e-03	3.02	1.52e-04	4.14	9.30e-04	3.50
4×4 Said-Ball	$[\frac{1}{2}, \frac{1}{2}]$	3.60e-03	–	2.18e-02	–	6.22e-03	–	4.98e-03	–
	$[\frac{1}{4}, \frac{1}{4}]$	9.35e-05	5.27	5.82e-04	5.23	2.50e-04	4.64	1.05e-04	5.56
	$[\frac{1}{8}, \frac{1}{8}]$	3.10e-06	4.91	1.97e-05	4.89	8.19e-06	4.93	3.44e-06	4.94

Tables 2 and 3 show that the conclusions in [18] are also applicable in this paper. Specifically, when the convection coefficient is time-independent, regardless of whether the stabilization parameter is related to the time or spatial step, the ERK-SUPG method proposed in Section 3 is effective. In addition, the calculated convergence orders clearly indicate that this method is effective for solving convection-dominated equations based on the error estimate (3.6) and (3.7) with $p = q + 1$.

Figures 4 and 6 respectively present solutions corresponding to stabilization parameters depending on the time and spatial step at $t = 1$. *The numerical solutions are obtained under the basis functions of degree* 3×3 *and* $1/8$ *partition. The left subplot shows the exact solution, the middle subplot depicts the numerical solution, and the right subplot displays the absolute error* ($|\mathbf{V}^n - u(\mathbf{x}, t_n)|$). *Both numerical methods for these parameters can effectively eliminate the nonphysical oscillations, and the numerical solution is highly consistent with the exact solution. This indicates that the ERK-SUPG method has stability and effectiveness when dealing with convection-dominated problems.*

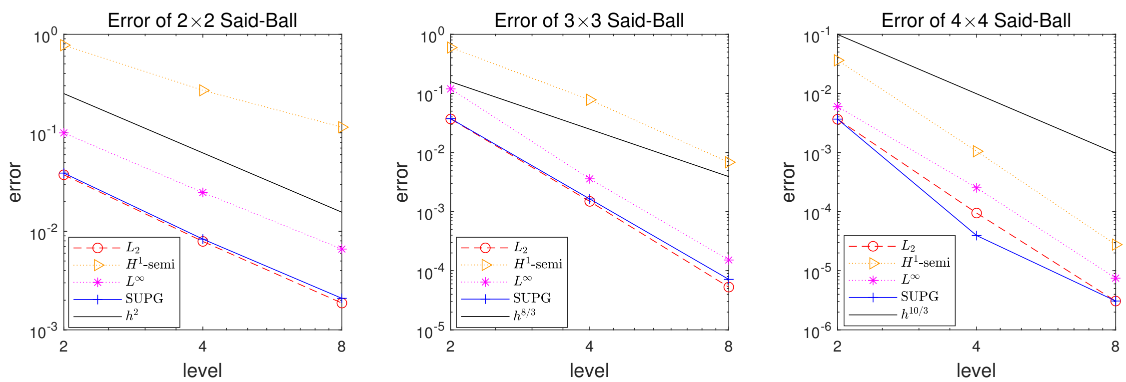

Figure 3. The numerical errors in Example 1 with $\delta_{\mathrm{M}} \sim \tau$.

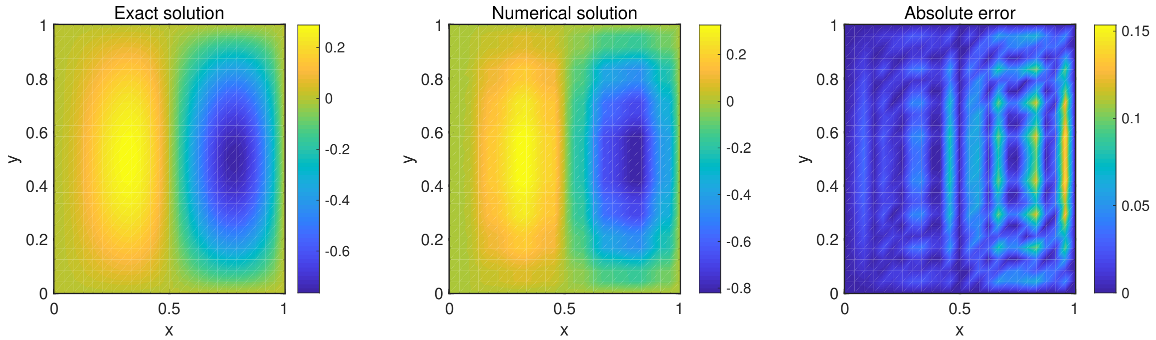

Figure 4. The comparison of the exact solution and numerical solution in Example 1 with $\delta_{\mathrm{M}} \sim \tau$.

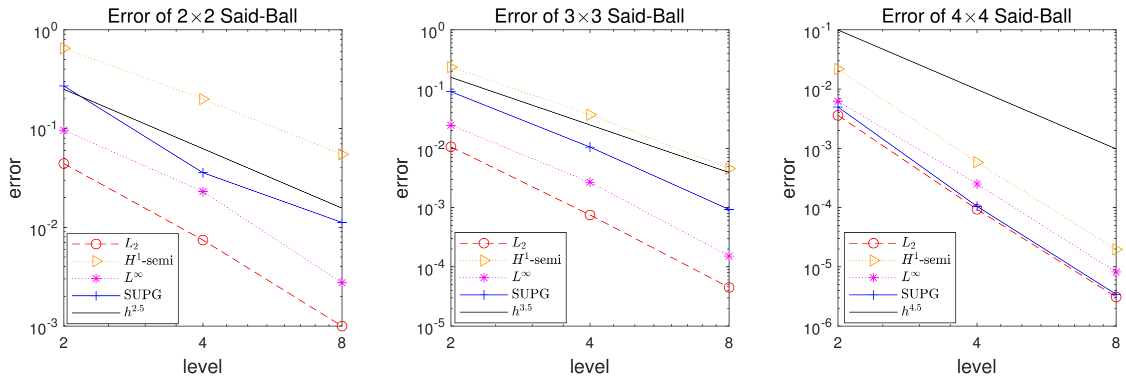

Figure 5. The numerical errors in Example 1 with $\delta_{\mathrm{M}} \sim h$.

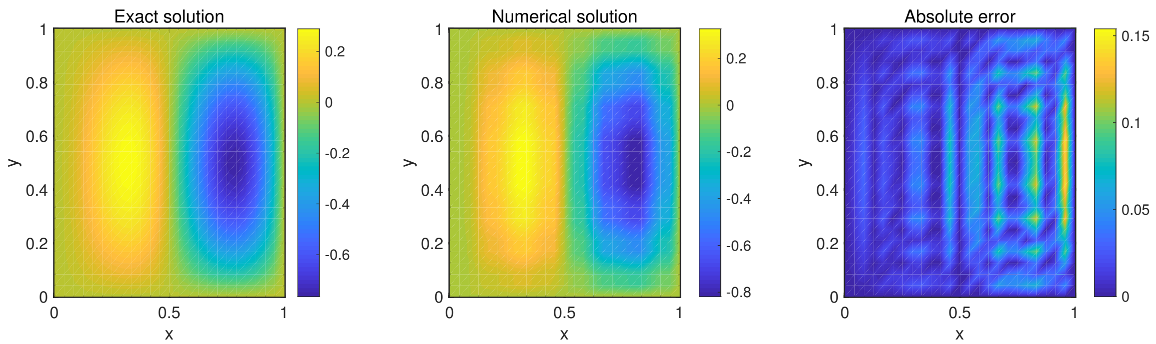

Figure 6. The comparison of the exact solution and numerical solution in Example 1 with $\delta_{\mathrm{M}} \sim h$.

Example 2. *The convection-dominated fluid migration process simulated by the CDR equations in this example corresponds to the transient dynamic response of the oil-gas two-phase flow in* $\Omega = [0,1] \times [0,1]$. *This scenario simulates the transient flow phase during the adjustment of injection and production parameters on offshore platforms.*

The diffusion coefficient is set to $\varepsilon = 10^{-7}$. *The time-dependent convection coefficient* $\mathbf{b} =$

$(1 + t,\ 5/3 + tsin(2\pi y))$ *is the actual seepage velocity. The reaction coefficient* $c = 1$ *quantifies the physicochemical interactions. The Dirichlet boundary condition stipulates that the concentrations of the oil and gas phases remain fixed throughout the simulation period. Further*

$$u(x, y, t) = t^2x^2y(1 - 3y + 2y^2)(x - 1),$$

and

$$\begin{aligned} f(x, y,t) = {} & (5/3 + tsin(2\pi y))(t^2x^2(x - 1)(2y^2 - 3y + 1) + t^2x^2y(4y - 3)(x - 1)) - 10^{-7}(4t^2x^2y(x - 1) \\ & + 2t^2x^2(4y - 3)(x - 1) + 4t^2xy(2y^2 - 3y + 1) - 2t^2y(x - 1)(2y^2 - 3y + 1)) \\ & + 2tx^2y(x - 1)(2y^2 - 3y + 1) + (1 + t)t^2xy(3x - 2)(2y^2 - 3y + 1) + t^2x^2y(x - 1)(2y^2 - 3y + 1). \end{aligned}$$

In this example, we use the 1×1*-,* 2×2*-, and* 3×3*-degree Said-Ball basis functions, respectively. When solving with* 3×3 *degree basis functions, due to the influence of computer precision, the minimum error can only be calculated to* 10^{-11}*. Let the stabilization parameter be* $\tau/8$*. In Table 4, we present the numerical errors and convergence orders obtained by the ERK-SUPG method described in Section 3. The errors corresponding to* 2×2 *degree basis functions are all smaller than those of* 1×1 *degree basis functions. The strong fitting ability of high-degree basis functions can more accurately characterize the oil and gas concentration. Meanwhile, with the refinement of mesh partitioning, the errors under both basis functions show a decreasing trend.*

Table 4. The numerical errors in Example 2.

Method	Mesh (h)	$\|\|\mathbf{V}^n - u(\mathbf{x}, t_n)\|\|$		$\|\mathbf{V}^n - u(\mathbf{x}, t_n)\|_1$		$\|\|\mathbf{V}^n - u(\mathbf{x}, t_n)\|\|_\infty$		$\|\|\mathbf{V}^n - u(\mathbf{x}, t_n)\|\|_{\mathrm{SUPG}}$	
		Error	Order	Error	Order	Error	Order	Error	Order
1×1 Said-Ball	$[\frac{1}{2}, \frac{1}{2}]$	6.97e-03	–	5.12e-02	–	1.49e-02	–	2.46e-02	–
	$[\frac{1}{4}, \frac{1}{4}]$	2.14e-03	1.70	2.92e-02	0.81	6.17e-03	1.27	7.27e-03	1.76
	$[\frac{1}{8}, \frac{1}{8}]$	5.24e-04	2.03	1.49e-02	0.97	2.16e-03	1.51	2.33e-03	1.64
	$[\frac{1}{16}, \frac{1}{16}]$	1.22e-04	2.11	7.20e-03	1.05	4.39e-04	2.30	7.07e-04	1.72
2×2 Said-Ball	$[\frac{1}{2}, \frac{1}{2}]$	9.80e-04	–	1.28e-02	–	2.51e-03	–	5.46e-03	–
	$[\frac{1}{4}, \frac{1}{4}]$	1.64e-04	2.58	3.66e-03	1.80	4.92e-04	2.35	8.84e-04	2.63
	$[\frac{1}{8}, \frac{1}{8}]$	2.40e-05	2.77	1.10e-03	1.73	7.48e-05	2.72	1.62e-04	2.45
	$[\frac{1}{16}, \frac{1}{16}]$	3.87e-06	2.65	3.59e-04	1.62	1.28e-05	2.55	3.01e-05	2.43
3×3 Said-Ball	$[\frac{1}{2}, \frac{1}{2}]$	6.17e-10	–	6.06e-09	–	1.73e-09	–	1.62e-09	–
	$[\frac{1}{4}, \frac{1}{4}]$	1.11e-10	–	6.06e-09	–	1.73e-10	–	2.30e-10	–
	$[\frac{1}{8}, \frac{1}{8}]$	2.61e-11	–	1.07e-09	–	1.01e-10	–	5.24e-11	–

Based on the theoretical result (3.6) obtained in the previous section, the final convergence order of the ERK-SUPG method is $2(q + 1)/3$ *for the* $q \times q$ *degree basis functions. Further, the convergence orders corresponding to the* 1×1 *degree and* 2×2 *degree basis functions are* $4/3$ *and* 2*, respectively, in Table 4 for the* L^2 *norm, which are consistent with the theoretical results.*

Figure 7 presents the exact solution, numerical solution, and absolute error ($|\mathbf{V}^n - u(\mathbf{x}, t_n)|$*) at* $t = 1$ *under* 1×1 *degree basis functions and* $1/16$ *partition. From this figure, it can be seen that the ERK-SUPG method can effectively suppress nonphysical oscillations and maintain a good consistency* *between the exact solution and the numerical solution. These results demonstrate that the ERK-SUPG method is stable and effective in simulating the transient convection-dominated two-phase migration process of oil and gas in offshore platforms.*

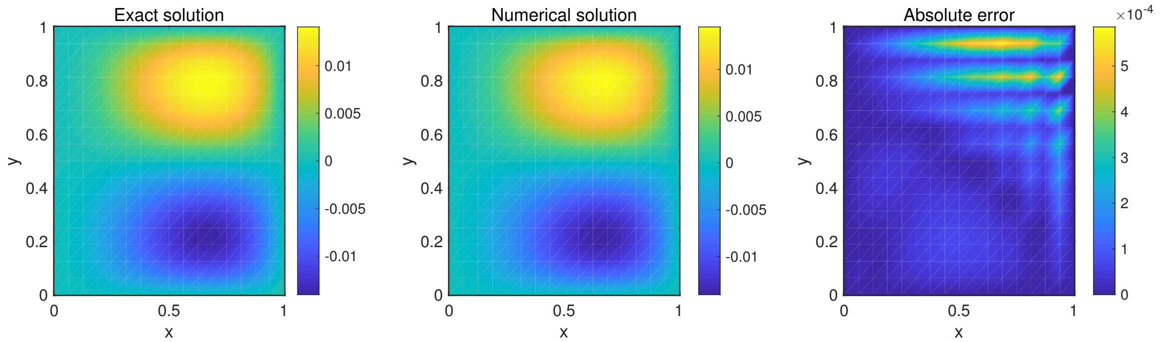

Figure 7. The comparison of the exact solution and numerical solution in Example 2.

Example 3. *In this example, the computational domain is set as* $\Omega = [0,1] \times [0,1]$*, specifically simulating the reservoir space around a cluster of production wells where oil-gas two-phase flow is concentrated. The convective coefficient* $\mathbf{b} = (7/10, 3/2)$ *corresponds to the stable driving effect generated by a steady pressure field during the mid-term production phase of offshore oilfields. The diffusion coefficient* $\varepsilon = 10^{-7}$ *represents the extremely weak fluid mixing process. The reaction coefficient* $c = 1$ *quantifies the rate of mild physicochemical interactions in stable flow conditions.*

The boundary at $y = 1$ *is set as a Neumann boundary with zero flux, representing an impermeable interface. The remaining boundaries are of Dirichlet type:* $x = 0$ *corresponds to a fluid inlet,* $x = 1$ *to an outlet, and* $y = 0$ *to a fixed bottom condition. This setup combines impermeable and fluid-exchange boundary conditions typical of convection-dominated transport problems. In addition,*

$$u(x,y,t) = t^3 sin(\pi x) sin(2\pi y),$$

and

$$f(x,y,t) = (3t^2 + t^3 + 5 \times 10^{-7} t^3 \pi^2) sin(\pi x) sin(2\pi y) + 3t^3 \pi cos(2\pi y) sin(\pi x) + 7/10\, t^3 \pi cos(\pi x) sin(2\pi y).$$

Because the convection term in this example is also time-independent, similar to Example 1, this example also calculates errors when the stabilization parameter is related to both the time step and the spatial step.

Tables 5 and 6 provide the errors and convergence orders when the stabilization parameters are related to the time step and spatial step, respectively. Among them, the stabilization parameters take $\tau/8$ *and* $h/4$*, respectively. From the data, it can be seen that as the degree of Said-Ball basis functions increases, the error decreases. When using* 3×3 *basis functions, the error decreases to* 10^{-7}*, which satisfies the accuracy requirements for fine-scale simulation of concentration gradients and fluid exchange. Comparing the convergence-order lines in Figure 8 and Figure 9 shows that the observed orders match theoretical predictions, confirming no numerical drift in long-term simulations and verifying the stability of the ERK-SUPG method.*

When the order p *of the ERK method is set to* $(q + 1)$*, and* $q \times q$ *degree basis functions are used, the theoretical convergence orders are* $2(q+1)/3$ *and* $(q+1/2)$ *for the* L^2 *norm. For instance, a* 4*-order ERK* *method combined with 3×3 ($q = 3$) degree basis functions yields the theoretical convergence orders of $8/3$ and 3.5. Further, the convergence orders in Tables 5 and 6 are consistent with the theoretical results. This means that the method accurately captures concentration evolution from fluid inlet to outlet while maintaining numerical rationality on impermeable and aquifer boundaries. Such behavior is consistent across all basis functions in Tables 5 and 6, further demonstrating the capability of the ERK-SUPG method to handle complex boundary conditions and deliver reliable numerical results.*

Table 5. The numerical errors in Example 3 by the ERK-SUPG method with $\delta_{\mathrm{M}} \sim \tau$.

Method	Mesh (h)	$\|\mathbf{V}^n - u(\mathbf{x}, t_n)\|$		$\|\mathbf{V}^n - u(\mathbf{x}, t_n)\|_1$		$\|\mathbf{V}^n - u(\mathbf{x}, t_n)\|_\infty$		$\|\mathbf{V}^n - u(\mathbf{x}, t_n)\|_{\mathrm{SUPG}}$	
		Error	Order	Error	Order	Error	Order	Error	Order
1×1 Said-Ball	$[\frac{1}{2}, \frac{1}{2}]$	6.93e-01	–	4.23e+00	–	1.75e+00	–	6.96e-01	–
	$[\frac{1}{4}, \frac{1}{4}]$	6.50e-02	3.41	1.61e+00	1.39	2.23e-01	2.97	7.01e-02	3.31
	$[\frac{1}{8}, \frac{1}{8}]$	1.27e-02	2.35	7.47e-01	1.11	4.37e-02	2.35	1.77e-02	1.99
	$[\frac{1}{16}, \frac{1}{16}]$	3.01e-03	2.08	3.69e-01	1.02	1.01e-02	2.11	6.75e-03	1.39
2×2 Said-Ball	$[\frac{1}{2}, \frac{1}{2}]$	7.27e-02	–	6.25e-01	–	1.30e-01	–	7.31e-02	–
	$[\frac{1}{4}, \frac{1}{4}]$	1.56e-02	2.22	9.75e-02	2.68	2.90e-02	2.17	1.57e-02	2.22
	$[\frac{1}{8}, \frac{1}{8}]$	1.96e-03	3.00	1.15e-02	3.08	3.94e-03	2.88	1.96e-03	3.00
	$[\frac{1}{16}, \frac{1}{16}]$	2.44e-04	3.00	1.35e-03	3.10	4.95e-04	2.99	2.45e-04	3.00
3×3 Said-Ball	$[\frac{1}{2}, \frac{1}{2}]$	5.22e-02	–	7.58e-01	–	1.80e-01	–	6.49e-02	–
	$[\frac{1}{4}, \frac{1}{4}]$	8.44e-04	5.95	5.62e-02	3.75	3.71e-03	5.60	1.26e-03	5.68
	$[\frac{1}{8}, \frac{1}{8}]$	1.43e-05	5.88	5.99e-03	3.23	3.09e-05	6.91	1.01e-04	3.64
	$[\frac{1}{16}, \frac{1}{16}]$	4.36e-07	5.03	7.25e-04	3.05	9.93e-07	4.96	1.21e-05	3.06

Table 6. The numerical errors in Example 3 by the ERK-SUPG method with $\delta_{\mathrm{M}} \sim h$.

Method	Mesh (h)	$\|\mathbf{V}^n - u(\mathbf{x}, t_n)\|$		$\|\mathbf{V}^n - u(\mathbf{x}, t_n)\|_1$		$\|\mathbf{V}^n - u(\mathbf{x}, t_n)\|_\infty$		$\|\mathbf{V}^n - u(\mathbf{x}, t_n)\|_{\mathrm{SUPG}}$	
		Error	Order	Error	Order	Error	Order	Error	Order
1×1 Said-Ball	$[\frac{1}{2}, \frac{1}{2}]$	5.14e-01	–	3.56e+00	–	1.08e+00	–	1.80e+00	–
	$[\frac{1}{4}, \frac{1}{4}]$	8.26e-02	2.64	1.48e+00	1.27	2.07e-01	2.39	5.39e-01	1.74
	$[\frac{1}{8}, \frac{1}{8}]$	1.50e-02	2.46	7.40e-01	1.00	3.89e-02	2.41	1.92e-01	1.49
	$[\frac{1}{16}, \frac{1}{16}]$	3.18e-03	2.24	5.68e-01	1.01	9.09e-03	2.10	6.75e-02	1.51
2×2 Said-Ball	$[\frac{1}{2}, \frac{1}{2}]$	6.55e-02	–	3.31e-01	–	1.35e-01	–	1.22e-01	–
	$[\frac{1}{4}, \frac{1}{4}]$	1.58e-02	2.06	7.36e-02	2.17	2.99e-02	2.18	2.19e-02	2.48
	$[\frac{1}{8}, \frac{1}{8}]$	1.96e-03	3.01	9.21e-03	3.00	4.03e-03	2.89	2.39e-03	3.20
	$[\frac{1}{16}, \frac{1}{16}]$	2.45e-04	3.00	1.16e-03	2.99	5.00e-04	3.01	2.73e-04	3.13
3×3 Said-Ball	$[\frac{1}{2}, \frac{1}{2}]$	1.56e-02	–	3.98e-01	–	3.50e-02	–	2.01e-01	–
	$[\frac{1}{4}, \frac{1}{4}]$	7.73e-04	4.33	3.81e-02	3.39	2.03e-03	4.11	1.42e-02	3.87
	$[\frac{1}{8}, \frac{1}{8}]$	4.88e-05	3.98	4.86e-03	2.97	1.55e-04	3.71	1.29e-03	3.46
	$[\frac{1}{16}, \frac{1}{16}]$	3.06e-06	4.00	6.11e-04	2.99	1.02e-05	3.93	1.14e-04	3.49

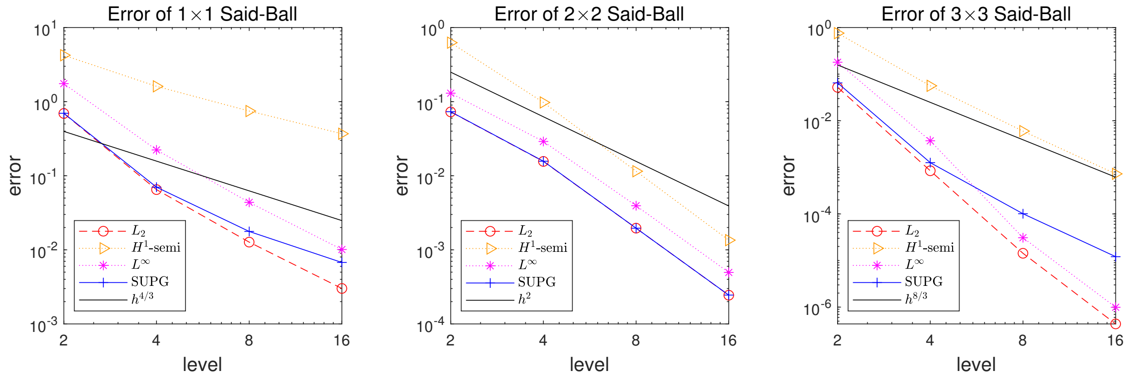

Figure 8. The numerical errors in Example 3 with $\delta_{\mathrm{M}} \sim \tau$.

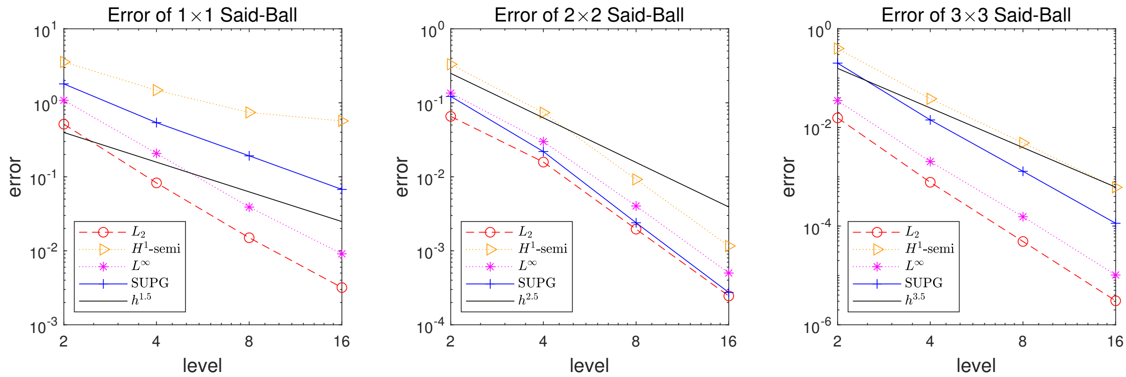

Figure 9. The numerical errors in Example 3 with $\delta_{\mathrm{M}} \sim h$.

In this section, these examples, with varied in boundary conditions and convection terms, demonstrate the method's effectiveness, thereby providing a reliable basis for selecting and parameterizing offshore reservoir simulation models.

5. Conclusions and future work

Solving convection-dominated CDR equations is essential for accurately capturing unsteady fluid transport. This work develops an ERK-SUPG scheme tailored for convection-dominated problems. For spatial discretization, we construct trial and test function spaces using Said-Ball basis functions of degree $q \times q$ within the SUPG framework; for time discretization, an m-stage p-order ERK method is utilized. We analyze the convergence rate and establish the optimal convergence orders. Extensive numerical tests on typical convection-dominated problems confirm that the presented ERK-SUPG method performs well when solving convection-dominated equations.

To summarize, the numerical framework established in this paper yields an accurate and efficient approach for modeling convection-dominated fluid transport in offshore reservoirs.

The extensions outlined below remain open for future investigation:

(1) Fractional PDEs will be investigated to capture anomalous diffusion and long-memory effects

inherent to reservoir fluid migration, which cannot be fully described by classical integer-order models.

(2) Numerical techniques defined over irregular domains will be explored to eliminate modeling errors introduced by simplified regular-domain assumptions and faithfully replicate real reservoir geometric features.
(3) We intend to integrate fractional differential operators with irregular domain constraints to strengthen the theoretical and numerical analysis of convection-dominated flows.

Upon completion, these follow-up studies will deliver higher-fidelity numerical tools for complex reservoir fluid simulation.

Author contributions

Lanyin Sun: Writing-review & editing, methodology, conceptualization, visualization, funding acquisition; Ziwei Dong: Writing-original draft, software, data curation. All authors have read and approved the final version of the manuscript for publication.

Use of Generative-AI tools declaration

The authors declare they have not used Artificial Intelligence (AI) tools in the creation of this article.

Acknowledgments

The authors are very grateful to the editor and anonymous referees for their valuable comments and constructive suggestions, which helped to improve the paper significantly. This work is partly supported by the Natural Science Foundation of Henan Province (No. 252300420348).

Conflict of interest

The authors declare that there is no conflict of interest.

References

1. L. Silva, C. Soares, Oilfield development system optimization under reservoir production uncertainty, *Ocean Eng.*, **225** (2021), 108758. https://doi.org/10.1016/j.oceaneng.2021.108758
2. J. Yang, The development and prospect of the offshore oil and gas industry, *Advances in Resources Research*, **1** (2021), 1–12. https://doi.org/https://doi.org/10.50908/arr.1.1_1
3. L. Silva, C. Soares, Optimisation of offshore oilfield development including the risk of failure of subsea manifolds, *Ocean Eng.*, **324** (2025), 120668. https://doi.org/10.1016/j.oceaneng.2025.120668
4. N. Babu, P. Lin, M. Abutaqiya, C. Sisco, J. Wang, F. Vargas, Systematic investigation of asphaltene deposition in the wellbore and near-wellbore region of a deepwater oil reservoir under gas injection, part 2: computational fluid dynamics modeling of asphaltene deposition, *Energy Fuels*, **33** (2019), 3645–3661. https://doi.org/10.1021/acs.energyfuels.8b03239

5. B. Wu, B. Zhang, Z. Jin, Multi-mechanism coupled dynamic modeling and numerical simulation of microbial enhanced oil recovery in heterogeneous oil reservoirs, *Advances in Resources Research*, **5** (2025), 2601–2631. https://doi.org/10.50908/arr.5.4_2601
6. A. Kim, Complete analytic solutions for convection-diffusion-reaction-source equations without using an inverse Laplace transform, *Sci. Rep.*, **10** (2020), 8040. https://doi.org/10.1038/s41598-020-63982-w
7. A. Askar, Á. Nagy, I. Barna, E. Kovács, Analytical and numerical results for the diffusion-reaction equation when the reaction coefficient depends on simultaneously the space and time coordinates, *Computation*, **11** (2023), 127. https://doi.org/10.3390/computation11070127
8. T. Ludescher, S. Gross, A. Reusken, A multigrid method for unfitted finite element discretizations of elliptic interface problems, *SIAM J. Sci. Comput.*, **42** (2020), A318–A342. https://doi.org/10.1137/18M1203353
9. P. Theeraek, S. Phongthanapanich, P. Dechaumphai, Solving convection-diffusion-reaction equation by adaptive finite volume element method, *Math. Comput. Simulat.*, **82** (2011), 220–233. https://doi.org/10.1016/j.matcom.2011.06.002
10. R. Lewis, A. Makurat, W. Pao, Fully coupled modeling of seabed subsidence and reservoir compaction of North Sea oil fields, *Hydrogeol. J.*, **11** (2003), 142–161. https://doi.org/10.1007/s10040-002-0239-z
11. M. Dunham, S. Ansari, C. Farquharson, Application of 3D marine controlled-source electromagnetic finite-element forward modeling to hydrocarbon exploration in the Flemish Pass Basin offshore Newfoundland, Canada, *Geophysics*, **83** (2018), WB33–WB49. https://doi.org/10.1190/geo2017-0451.1
12. R. Allawi, M. Al-Jawad, 4D Finite element modeling of stress distribution in depleted reservoir of south Iraq oilfield, *J. Petrol. Explor. Prod. Technol.*, **12** (2022), 679–700. https://doi.org/10.1007/s13202-021-01329-5
13. T. Russell, Time stepping along characteristics with incomplete iteration for a Galerkin approximation of miscible displacement in porous media, *SIAM J. Numer. Anal.*, **22** (1985), 970–1013. https://doi.org/10.1137/0722059
14. E. do Carmo, G. Alvarez, A new stabilized finite element formulation for scalar convection-diffusion problems: the streamline and approximate upwind/Petrov-Galerkin method, *Comput. Method. Appl. Mech.*, **192** (2003), 3379–3396. https://doi.org/10.1016/S0045-7825(03)00292-5
15. E. Parish, M. Yano, I. Tezaur, T. Iliescu, Residual-based stabilized reduced-order models of the transient convection-diffusion-reaction equation obtained through discrete and continuous projection, *Arch. Computat. Methods Eng.*, **32** (2025), 1885–1929. https://doi.org/10.1007/s11831-024-10197-1
16. A. Brooks, T. Hughes, Streamline upwind/Petrov-Galerkin formulations for convection dominated flows with particular emphasis on the incompressible Navier-Stokes equations, *Comput. Method. Appl. Mech.*, **32** (1982), 199–259. https://doi.org/10.1016/0045-7825(82)90071-8
17. T. Tezduyar, Y. Park, H. Deans, Finite element procedures for time-dependent convection-diffusion-reaction systems, *Int. J. Numer. Meth. Fl.*, **7** (1987), 1013–1033. https://doi.org/10.1002/fld.1650071003

18. V. John, J. Novo, Error analysis of the SUPG finite element discretization of evolutionary convection-diffusion-reaction equations, *SIAM J. Numer. Anal.*, **49** (2011), 1149–1176. https://doi.org/10.1137/100789002
19. M. Esmaily, D. Jia, An augmented streamline upwind/Petrov-Galerkin method for the time-spectral convection-diffusion equation, *J. Comput. Phys.*, **520** (2025), 113484. https://doi.org/10.1016/j.jcp.2024.113484
20. C. Provatidis, Bézier versus Lagrange polynomials-based finite element analysis of 2-D potential problems, *Adv. Eng. Softw.*, **73** (2014), 22–34. https://doi.org/10.1016/j.advengsoft.2014.02.006
21. M. Bacciocchi, N. Fantuzzi, Free vibrations and bending of laminated thin plates with distorted domains in gradient elasticity: an isoparametric finite element formulation based on Hermite mapping, *Acta Mech.*, in press. https://doi.org/10.1007/s00707-025-04254-4
22. A. Rodríguez, L. Bruno, F. Rapetti, Whitney edge elements and the Runge phenomenon, *J. Comput. Appl. Math.*, **427** (2023), 115117. https://doi.org/10.1016/j.cam.2023.115117
23. G. Hu, M. Li, J. Zhong, Combined cubic generalized Ball surfaces: construction and shape optimization using an enhanced JS algorithm, *Adv. Eng. Softw.*, **176** (2023), 103404. https://doi.org/10.1016/j.advengsoft.2022.103404
24. S. Zafar, M. Hussain, Fair curve designing by Said-Ball curve, *PLoS One*, **20** (2025), e0324553. https://doi.org/10.1371/journal.pone.0324553
25. H. Wu, Dual bases for a new family of generalized Ball bases, *J. Comput. Math.*, **22** (2004), 79–88.
26. L. Zhang, H. Wu, J. Tan, Dual bases for Wang-Bézier basis and their applications, *Appl. Math. Comput.*, **214** (2009), 218–227. https://doi.org/10.1016/j.amc.2009.03.079
27. G. Hu, W. Dou, B. Du, Degree reduction of ball Said-Ball surfaces using an enhanced coot optimization algorithm, *Math. Method. Appl. Sci.*, **48** (2025), 8297–8321. https://doi.org/10.1002/mma.9791
28. A. Stuart, A. Peplow, The dynamics of the theta method, *SIAM Journal on Scientific and Statistical Computing*, **12** (1991), 1351–1372. https://doi.org/10.1137/0912074
29. B. Sanderse, B. Koren, Accuracy analysis of explicit Runge-Kutta methods applied to the incompressible Navier-Stokes equations, *J. Comput. Phys.*, **231** (2012), 3041–3063. https://doi.org/10.1016/j.jcp.2011.11.028
30. I. Faragó, Convergence and stability constant of the theta-method, *Proceedings of Applications of Mathematics 2013*, 2013, 42–51.
31. S. Keeling, Galerkin/Runge-Kutta discretizations for semilinear parabolic equations, *SIAM J. Numer. Anal.*, **27** (1990), 394–418. https://doi.org/10.1137/0727024
32. M. Song, Z. Yang, M. Liu, Stability of θ-methods for advanced differential equations with piecewise continuous arguments, *Comput. Math. Appl.*, **49** (2005), 1295–1301. https://doi.org/10.1016/j.camwa.2005.02.002
33. J. Butcher, A history of Runge-Kutta methods, *Appl. Numer. Math.*, **20** (1996), 247–260. https://doi.org/10.1016/0168-9274(95)00108-5
34. Z. Sun, C. Shu, Strong stability of explicit Runge-Kutta time discretizations, *SIAM J. Numer. Anal.*, **57** (2019), 1158–1182. https://doi.org/10.1137/18M122892X

35. C. Runge, Über die numerische Auflösung von differentialgleichungen, *Math. Ann.*, **46** (1895), 167–178. https://doi.org/10.1007/BF01446807

36. J. Butcher, Implicit Runge-Kutta processes, *Math. Comp.*, **18** (1964), 50–64. https://doi.org/10.1090/S0025-5718-1964-0159424-9

37. R. Alexander, Diagonally implicit Runge-Kutta methods for stiff ODE's, *SIAM J. Numer. Anal.*, **14** (1977), 1006–1021. https://doi.org/10.1137/0714068

38. G. Dimarco, L. Pareschi, Asymptotic preserving implicit-explicit Runge-Kutta methods for nonlinear kinetic equations, *SIAM J. Numer. Anal.*, **51** (2013), 1064–1087. https://doi.org/10.1137/12087606X

39. F. Ghoreishi, R. Ghaffari, N. Saad, Fractional order Runge-Kutta methods, *Fractal Fract.*, **7** (2023), 245. https://doi.org/10.3390/fractalfract7030245

40. L. Sun, Z. Dong, A θ-difference finite element method for solving convection-diffusion-reaction equations based on the Wang-Ball element, *J. Appl. Math. Comput.*, **71** (2025), 7639–7673. https://doi.org/10.1007/s12190-025-02556-3

41. L. Zhang, J. Tan, Z. Dong, The dual bases for the Bézier-Said-Wang type generalized Ball polynomial bases and their applications, *Appl. Math. Comput.*, **217** (2010), 3088–3101. https://doi.org/10.1016/j.amc.2010.08.041

42. P. Ciarlet, *The finite element method for elliptic problems*, Philadelphia: Society for Industrial and Applied Mathematics, 2002. https://doi.org/10.1137/1.9780898719208

43. H. Roos, M. Stynes, L. Tobiska, *Robust numerical methods for singularly perturbed differential equations: convection-diffusion-reaction and flow problems*, Berlin: Springer, 2008. https://doi.org/10.1007/978-3-540-34467-4

44. C. Lubich, A. Ostermann, Runge-Kutta approximation of quasi-linear parabolic equations, *Math. Comp.*, **64** (1995), 601–627. https://doi.org/10.1090/S0025-5718-1995-1284670-0

45. Q. Zhang, C. Shu, Stability analysis and a priori error estimates of the third order explicit Runge-Kutta discontinuous Galerkin method for scalar conservation laws, *SIAM J. Numer. Anal.*, **48** (2010), 1038–1063. https://doi.org/10.1137/090771363